Int J Adv Manuf Technol (2016) 85:1983–1993
DOI 10.1007/s00170-015-7999-9

ORIGINAL ARTICLE

Spark radius modeling of resistance-capacitance pulse discharge in micro-electric discharge machining of Ti-6Al-4V: an experimental study

B. Kuriachen[1] · **Jose Mathew**[2]

Received: 29 April 2015 / Accepted: 20 October 2015 / Published online: 29 October 2015

Abstract Several modeling and simulations have been reported to characterize the electric discharge machining (EDM) and micro-electric discharge machining (micro-EDM) processes. However, these models have been considered spark radius as a function of time or time and current as well as these models are valid only for transistor-type pulse discharge circuits. Therefore, it is important to develop an accurate model to predict the spark radius for RC-relaxation circuits where capacitance and voltage are the important process parameters. In this paper, an attempt has been made to develop a mathematical model predicting the single-spark radius produced during micro-EDM of Ti-6Al-4V. A series of experiments were conducted based on three-level full factorial experimental design with four center point runs. Capacitance and voltage were taken as the variable factors and spark radius was measured as the response. Based on the experimental results, the effect of capacitance and voltage on spark radius was studied in detail with analysis of variance. The results showed that capacitance significantly influenced the spark radius compared to voltage. In addition, a mathematical model has been developed to correlate the capacitance and voltage with spark radius by adopting regression analysis. Finally, the developed model equation was validated with confirmatory experiments and the predicted and experimental spark radius was found to be in good agreement with a prediction error less than 5 %.

Keywords Micro-EDM · Ti-6Al-4V · Spark radius · Modeling · RC-circuit · Surface modification

1 Introduction

Nowadays, meso (1–10 mm) and micro (1–1000 μm) manufacturing are emerging as an important technology especially in the areas where miniaturization yields economic and technical benefits namely, aerospace, automotive, optical, biomedical, and other similar areas. Micro-manufacturing of advanced materials by means of conventional micro-manufacturing techniques are extremely difficult due to the improved mechanical properties. Hence, the advanced manufacturing techniques have to be developed in order to meet the increased demand in processing the advanced materials.

Electric discharge machining (EDM) is an advanced manufacturing process which can machine any electrically conductive materials regardless of its hardness. It removes materials from the work piece by means of rapid and repetitive spark discharges [1]. The high temperature generated in the inter electrode gap due to electron collision melts and vaporizes small portion of material from both electrodes. Micro-EDM has similar working principle and characteristics as that of EDM except for the size of the tool electrode and discharge energy.

Nowadays, titanium and its alloys are extensively used in aerospace, medical, marine, and automobile industries because of its improved mechanical properties and biocompatibility. Machining of titanium alloys are extremely difficult in conventional machining due to its low thermal conductivity

✉ B. Kuriachen
basilkuriachen@gmail.com

Jose Mathew
josmat@nitc.ac.in

[1] School of Mechanical and Building Sciences, VIT University, Vellore, India

[2] Department of Mechanical Engineering, National Institute of Technology Calicut, Kerala, India

and low modulus of elasticity, which causes significant spring back after deformation under the machining load. Therefore, micro-EDM is one of the best suited processes for the micromachining of titanium and its alloys [2]. Secondly, EDM has been used for machining electrically conductive materials for many years; however, the material removal mechanism is not fully understood because of the stochastic and complex nature of the sparks. To understand this phenomenon, researchers have used many methods.

Jilani and Pandey [3] proposed a two-dimensional heat transfer model, with disc heat source to study the effects of EDM input parameters, such as pulse duration, pulse energy, and material properties, on material removal and crater shape. It showed poor correlation between theoretical and experimental data. A simple cathode erosion model for conventional EDM was developed by Dibitonto et al. [4]. In this, photoelectric effect was considered as the dominant source of energy supplied to cathode surface. Patel et al. [5] presented an anode erosion model which accepts power rather than temperature as the boundary condition at the plasma/anode interface. The power supplied is assumed to produce a Gaussian-distributed heat flux on the surface of the anode material, and the area upon which the flux is incident is assumed to grow with time. A fundamental study of EDM based on the physics of an arc and heat transfer theory was carried out by Shankar et al. [6]. The field equations for electric potential and temperature in the spark region were solved to calculate the final spark shape and the percentage of heat absorbed by cathode, anode, and dielectric. Another model based on electrostatic force acting on the surface of work piece for short pulses was introduced by Ajit and Ghosh [7]. They have found out the electrostatic force acting on the metal surface and its influence on the stress distribution inside the metal thereby the crater depth. In modeling and simulation of micro-EDM process, Rajurkar et al. [8] developed a mathematical model of contouring EDM process considering the profile of workpiece, actual tool path, and machined surface profile. Dhanik and Joshi [9] presented a model of a single-resistance pulse discharge in micro-electric discharge machining. This comprehensive model incorporated various phenomena in the pre-breakdown period and considered plasma as a time variable source of energy to the cathode and anode. Marafona and Chousal [10] presented a finite element model of EDM based on Joule effect. The radii value of the conductor is assumed to be the function of current intensity and pulse duration. Joshi and Pande [11] proposed an intelligent model for the EDM process using finite element method (FEM) and artificial neural network. They considered Gaussian distribution of heat flux, time, and energy-dependent spark radius, etc. to predict the shape of crater cavity, material removal rate, and tool wear rate. Izquierdo et al. [12] contributed to the simulation and modeling of EDM process with multiple discharges using a finite difference method. The material removal in EDM is modeled as a thermal problem where the objective is to determine the temperature distribution in the work piece from the discharges. Joshi and Pande [13] developed a single-spark thermo physical model for die-sinking electric discharge machining using 2D finite element method. It was based on more realistic assumptions such as Gaussian distribution of heat flux, spark radius equation based on discharge current and discharge duration, latent heat of melting, etc. Chang [14] modeled EDM process considering axisymetric process continuum, Gaussian distribution of heat flux, spark radius based on discharge current and discharge duration, latent heat of melting, and percentage of discharge energy transferred to work piece to predict the shape of the crater. Shabgard et al. [15] presented the temperature distribution on the surface of work piece and tool during a single-discharge EDM process using FEM. Based on the results of FEM and experimental observations, a numerical analysis has been performed to assess the contribution of input parameters on the efficiency of plasma channel in removing the molten material from work piece and tool at the end of each discharges. Recast layer distribution in EDM of inconel 718 has been simulated by Izquierdo et al. [16] and predicted the recast layer with less than 4.5 μm using FEM. Zhang et al. [17] proposed a novel method of determining the energy distribution and plasma diameter of EDM by comparing the boundary of the melted material obtained from metallographic and finite element method. They have investigated the energy distribution and plasma diameter in different dielectrics with different polarities. Comparison between the results and the previous reported results showed that the energy distributed into work piece and plasma diameter can be determined by this new method. Different approaches [18–22] for solving the thermal process of EDM can be found in literature, and its developments towards modeling of micro-EDM are presented by S. Dhanik et al. [23].

Yu et al. [24] have introduced an analytical model for micro-EDM to investigate the effect of tool wear, and it is verified using micro- and macro-EDM of slots. Murali and Yeo [25] developed a single-spark model for micro-EDM of titanium alloy. To estimate the crater size, temperature distribution on the work piece, and residual stress on and near the crater, a transient thermal analysis had been done using commercially available finite element method. Simulated crater dimensions and residual stresses were compared with experimentally obtained values by atomic force microscope (AFM) and nanoindentation technique. Yeo et al. [26] proposed an analytical model based on electrothermal theory to estimate the geometrical dimensions of micro-crater. The model incorporates voltage, current, and pulse-on-time during material removal to predict the temperature distribution on AISI 4140 alloy steel as a result of single discharges in micro-EDM. The experimental and theoretical results are found to be in close agreement till 1000 ns of pulse on time. Kiran and Joshi [27]

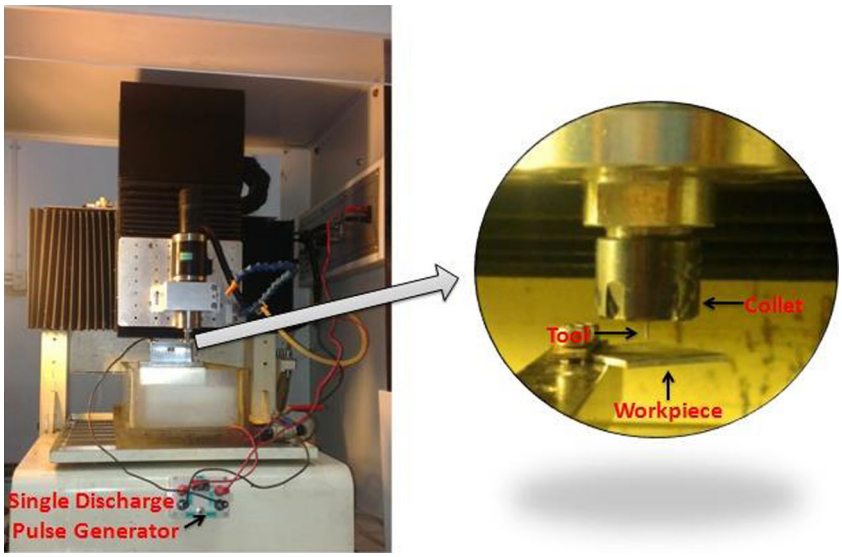

Fig. 1 Experimental set up

presented a model to predict surface roughness of micro-ED machined surfaces based on the configuration of a single-spark cavity formed as a function of process parameters. Normal distribution of the surface heights was assumed and μ and σ (R_q) of the surface profiles are evaluated after spark. The model is further extended to investigate the role of debris inclusion in the dielectric using chemical kinetics approach. Allen and Chen [28] presented the results of process simulation and residual stress analysis for the micro-EDM on molybdenum. Material removal is analyzed using a thermo-numerical model for single-spark discharge process. A coupled thermo-structural finite element analysis was also presented to study how the thermal action of the micro-EDM process affected the surface integrity of machined work piece. Three-dimensional FEM model of micro-EDM was developed by Mathew et al. [29] and analyzed the effect of Gaussian heat flux on inconel 718 while machining. Somashekar et al. [30] presented numerical results based on electrothermal theory using finite element method for single discharge. The single-spark model was developed, based on more realistic assumptions such as Gaussian distribution of heat flux, time and energy-dependent spark radius, etc. to predict the shape of crater cavity, material removal rate, and tool wear rate. They have extended this approach with multi-spark numerical model based on 2D finite volume method [31] and predicted the effect of spark ratio on the temperature distribution in the work piece. Tan et al. [32] developed a model for overlapping craters.

Among the various approaches to model the EDM/micro-EDM, numerical simulation is widely used to study the process. During the numerical simulation of the electric sparks, most of the researchers have used spark radius as time-dependent function [12, 13] or both time and current dependent [11, 15]. But, the discharge energy for RC pulse discharge circuit is decided by capacitance and voltage (E= 0.5C V^2). The function of the capacitor is to store the charge till the voltage reaches the breakdown voltage and then discharge it in the form of a spark or pulse. The higher the capacitance, the larger will be the amount of charge stored and greater will be the discharge duration. Hence, both the pulse current and duration of discharges are imperative parameters for RC micro-EDM process which are decided by capacitance

Table 1 Chemical composition of work material

Chemical composition of Ti-6Al-4V (wt. %)	
Ti	Balance
Al	5.5–6.67
V	3.5–4.5
Fe	<0.25
O	<0.2
C	<0.08
N	<0.05

Table 2 Mechanical and physical properties of Ti-Al-4V

Properties	Value
Melting range °C±15	1649
Specific heat (J/kg °C)	560
Volume electrical resistivity (ohm cm)	170
Thermal conductivity (W/mK)	7.2
Ultimate tensile strength (MPa)	832
Coefficient of linear thermal expansion (μm/m °C)	8.6

Table 3 Machining parameters with their levels for micro-EDM process

Parameter	Levels		
	−1	0	1
Capacitance (nF)	1	1000	2200
Gap voltage (V)	80	115	150

and voltage [33, 34]. Jahan et al. [35] compared transistor and RC-type pulse generator for machining fine quality micro-holes. They reported that RC-type pulse generators are best suited for micro-EDM. Thus, a need exists to model the spark radius of RC micro-EDM in terms of the process parameters such as capacitance and voltage.

In the present paper, an attempt has been made to model the complex micro-EDM process experimentally. The effect of important RC micro-EDM process parameters such as voltage (V) and capacitance (C) on Ti-6Al-4V is investigated. Initially, the experiments based on the three-level full factorial designs were conducted at various levels. The second phase involves the analysis and investigates the level of significance of each process parameters as well as its interaction effect on spark radius. Finally, a mathematical model to predict the spark radius in terms of capacitance and voltage was developed and validated with confirmation experiments.

2 Experimental details

2.1 Machine tool

The experiments were conducted using a multipurpose machine tool developed by MIKROTOOLS Pte. Ltd., Singapore, Model: DT-110, for high-precision micromachining. It is energized by a pulse generator which can be switched to both transistor type and RC type. The maximum travel range of the machine is 200 mm (X)× 100 mm (Y)×100 mm (Z) with a resolution of 0.1 μm in X, Y, and Z directions; Fig. 1 shows the experimental set up.

2.2 Work piece and electrode

The work piece and tool electrode materials used in this study were Ti-6Al-4V and tungsten carbide of diameter 0.4 mm, respectively. The important composition and properties of the work piece are listed in Tables 1 and 2, respectively.

2.3 Experimental procedure

Before experimentation, to make the work piece free from all sorts of scratches, it was polished with different grades of emery paper, namely 320, 400, 600, and finally with diamond

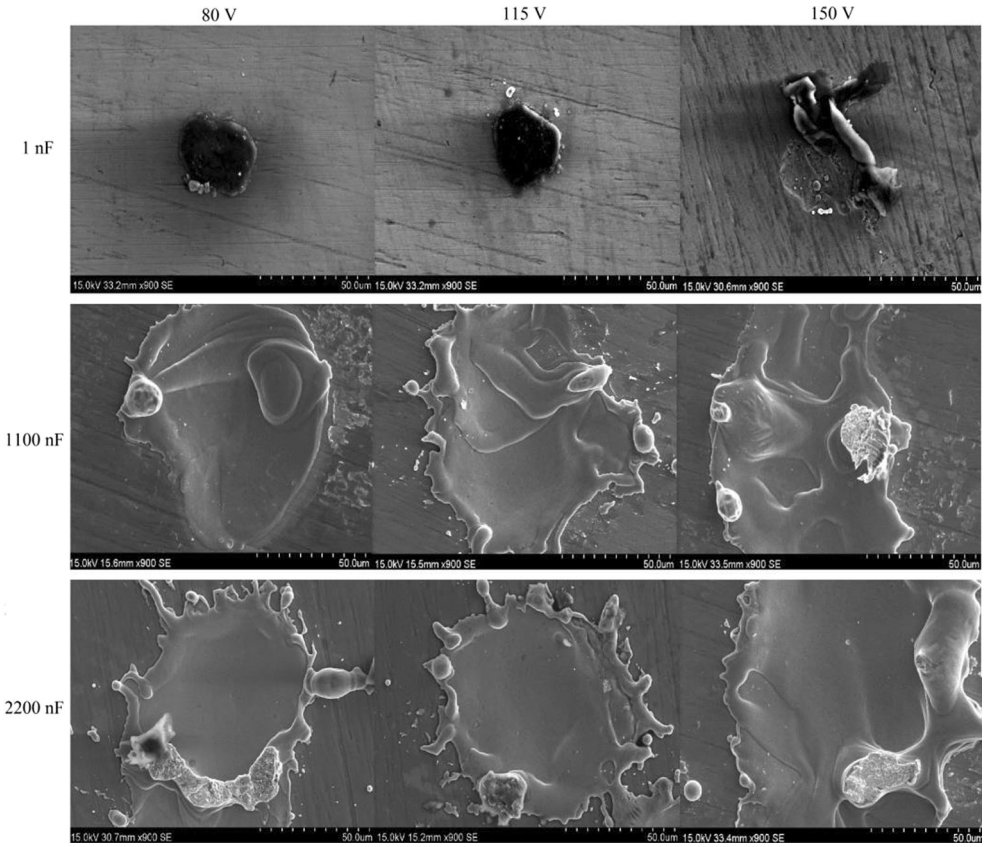

Fig. 2 SEM images of single-spark crater

Table 4 Experimental design and output response

Std. Order	Run Order	Capacitance (nF)	Voltage (V)	Diameter (μm)	Radius (μm)
1	7	1	80	32.47	16.235
2	3	1100.5	80	91.27	45.635
3	11	2200	80	78.66	39.33
4	12	1	115	32.42	16.21
5	2	1100.5	115	98.06	49.03
6	10	2200	115	89.33	44.665
7	13	1	150	32.4	16.2
8	5	1100.5	150	94.833	47.4165
9	6	2200	150	124	62
10	1	1100.5	115	110.67	55.335
11	4	1100.5	115	81	40.5
12	8	1100.5	115	95.86	47.93
13	9	1100.5	115	97.467	48.7335

paste in double disc polishing machine. The experiments were designed based on three-level full factorial design in order to observe the individual as well as the interaction effects of different process parameters on spark radius. A total number of 13 experiments were conducted, which included four repeated center runs. The experiments were conducted in a random order so as to remove the effects of any unaccounted factors. At the end of each experiment, the work piece was removed and spark diameter was measured using scanning electron microscope. The different process parameters and their levels in coded and actual values are shown in Table 3. The design was generated and analyzed using commercially available Design-Expert software package.

3 Results and discussion

The radius of the single-spark craters on Ti-6Al-4V were measured using scanning electron microscope with an accelerating voltage of 15.0 kV. The observed images for all the samples have been depicted in Fig. 2. The experimental design and results for spark diameter are tabulated in Table 4. Analysis of variance (ANOVA) was used to identify the level of significance of each process parameters and their interactions. Results of the analysis are discussed in the following sections.

3.1 Analysis of spark radius

The ANOVA for spark radius is performed with the help of Design-Expert software. Table 5 shows the effect of individual and interaction effect of the developed model for spark radius. The model is developed at 95 % confidence level of significance. The model F value of 30.227 implies that the model is significant with negligible influence of noise. From the results, it has been observed that capacitance is the most significant factor for spark radius. In addition to capacitance, model terms AB (interaction of capacitance and voltage) and A^2 (quadratic term of capacitance) are significant with a "Prob> F" less than 0.05. The R^2 value of 0.9379, Adj R^2 of 0.9069, Pred R^2 of 0.8073, and Adeq Precisior of 15.320 showed the dependency of the model. The Pred R^2 and Adj R^2 are in reasonable agreement with a difference of 0.1. Figure 3 shows the effect of capacitance on spark radius. It is observed that spark radius is more sensitive to capacitance than voltage. The

Table 5 ANOVA for spark radius

Source	Sum of square	df	Mean square	F value	p value Prob>F
Model	2569.6	4	642.42	30.227	<0.0001
A	1579.5	1	1579.5	74.318	<0.0001
B	99.36	1	99.361	4.67508	0.0626
AB	128.8	1	128.88	6.06396	0.0392
A^2	761.9	1	761.95	35.8509	0.0003
Resi.	170.0	8	21.253		

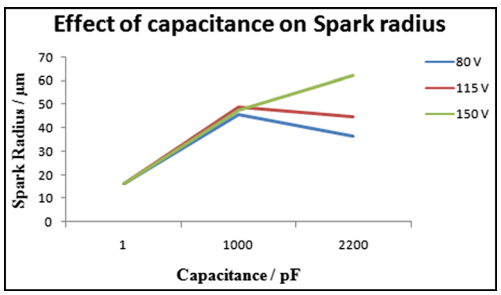

Fig. 3 Capacitance vs spark radius

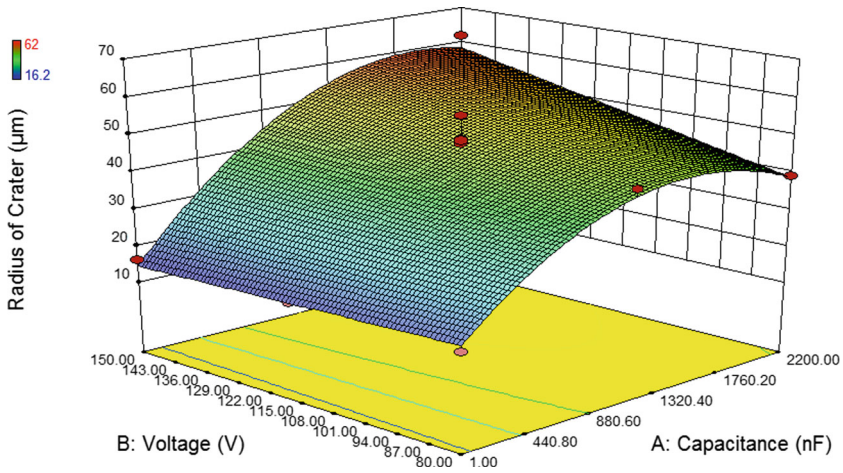

(a) 3D surface plot

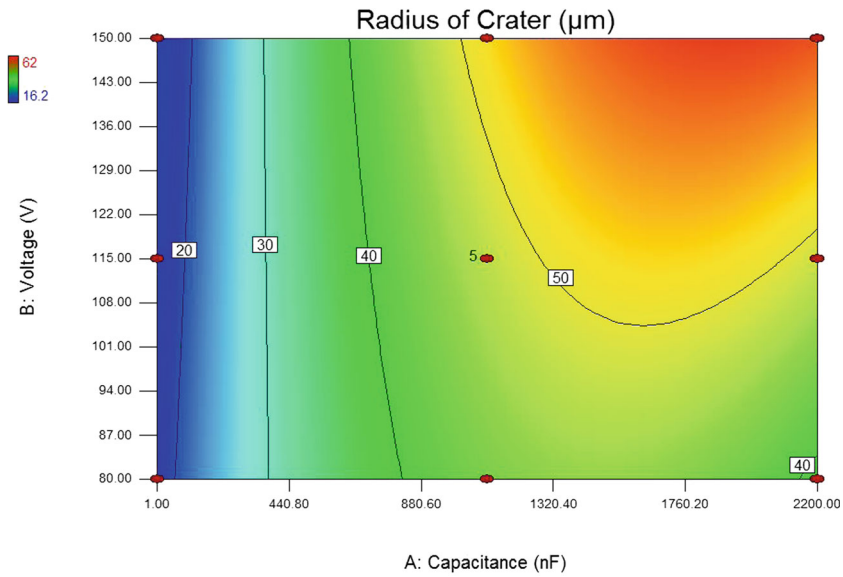

(b) Contour plot

Fig. 4 **a** 3D surface plot. (**b**) Contour plot for capacitance voltage interaction

function of the capacitor is to store the charge till the voltage reaches the breakdown voltage and then discharge it in the form of a spark or pulse. With increase in capacitance, larger energy is being dissipated which produces stronger sparks thereby larger spark radius. Spark radius increases, as the capacitance increases, but for 115 V and 80 V, spark radius decreased a little at the highest level of capacitance. At these levels double sparking was observed.

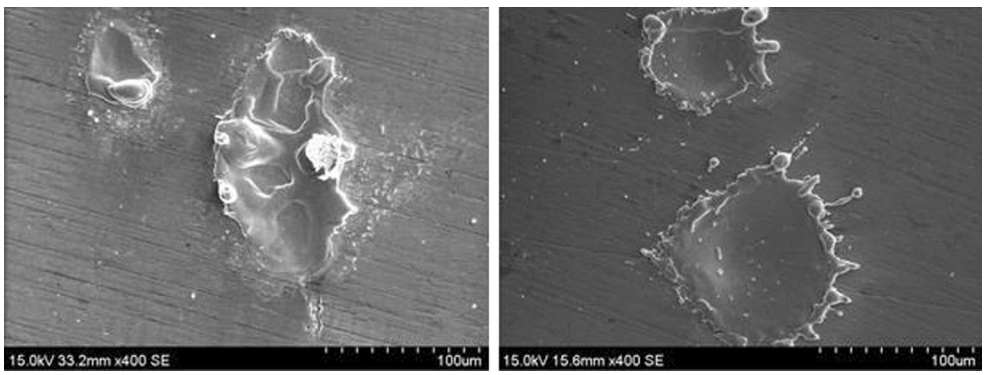

Fig. 5 SEM images of double sparks

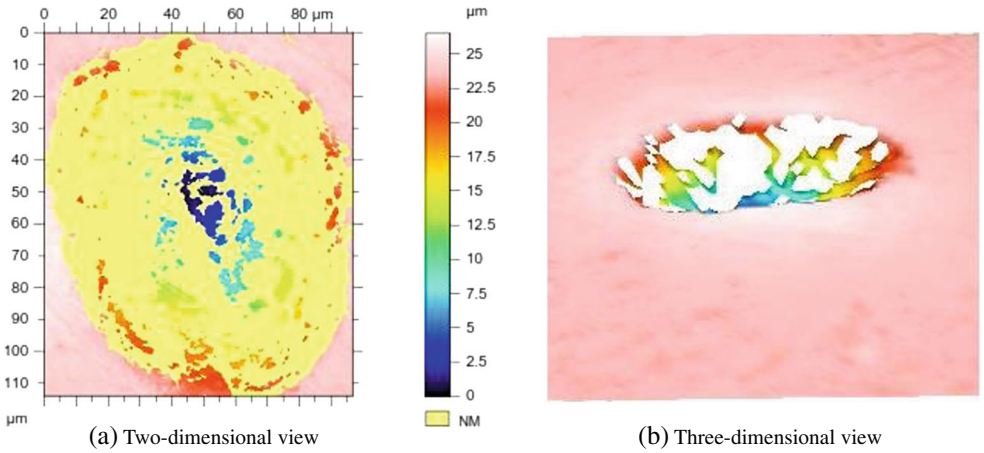

(a) Two-dimensional view (b) Three-dimensional view

Fig. 6 Scanned craters at 2.2 µF and 80 V. **a** Two-dimensional view. **b** Three-dimensional view

Figure 4 shows the 3D surface plot and the contour plot for spark radius in terms of process parameters. From these graphs, it is again confirmed that spark radius is more sensitive to capacitance than voltage. It increases up to an optimum level, there after it decreases; this is due to the double sparking which occurred in the interelectrode gap at high discharge energies, thereby the energy is divided among the two sparks unevenly. As the capacitance increases, the charge stored in the capacitor also increases, thereby the charging time increases whereas discharge time remains the same. As a result, more energy gets release into the interelectrode gap. In actual practice, both the electrode surfaces contain peaks and valleys. The ionization channel gets formed where ever the optimum gap is achieved during the discharge time. Due to the high

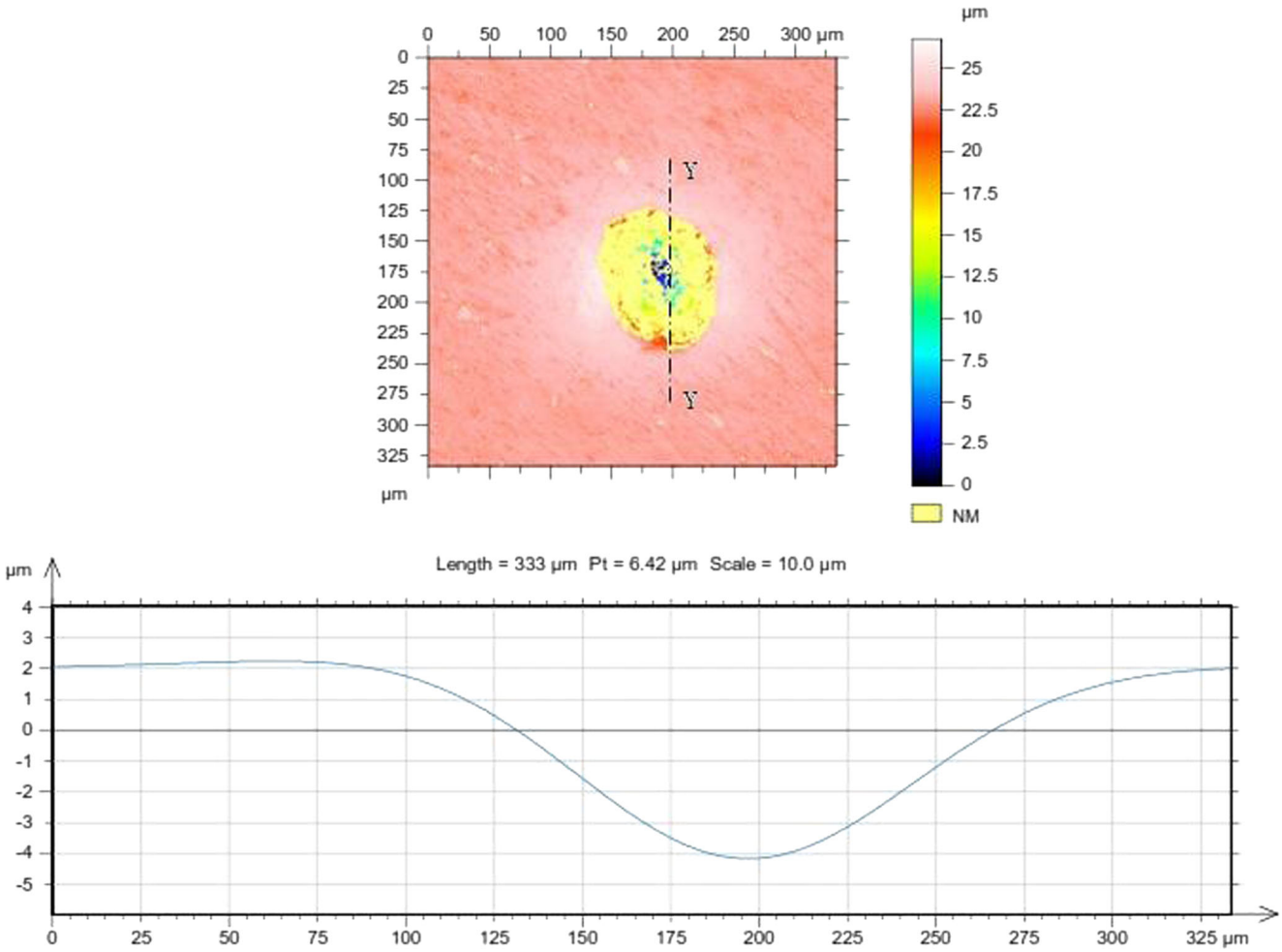

Fig. 7 Carter shape at section Y-Y: experimental results at 2200 nF and 80 V

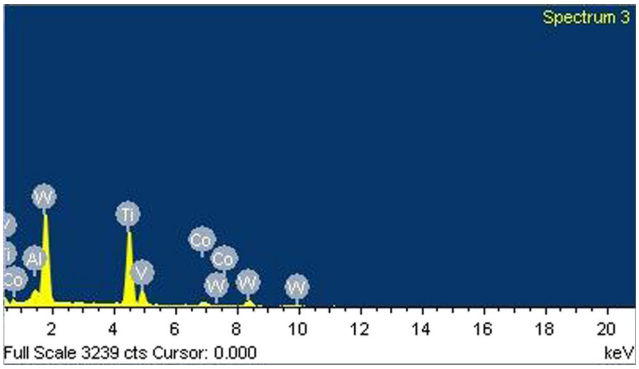

Fig. 8 EDS analysis of single-spark crater

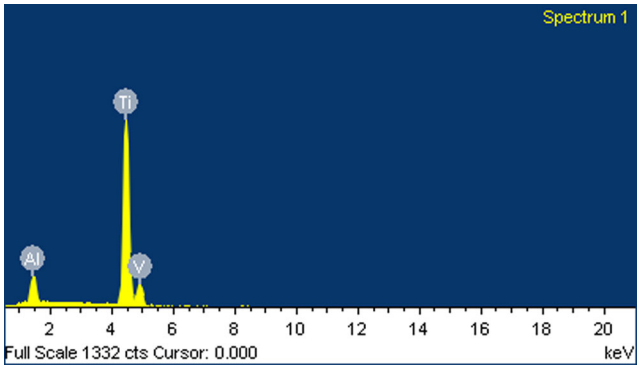

Fig. 9 EDS composition analysis of unprocessed Ti-6Al-4V surface

energy release into the discharge gap, there are some possibilities to form two or more ionization channels which is having different diameter (due to the difference in the optimum inter electrode gap) to discharge the stored energy completely. Hence, before the full energy get released into the interelectrode gap, the next spark occurs in the second smallest distance between the tool and work piece. Therefore, the remaining energy is discharged as a secondary spark. In the case of further increase in energy during discharge time may lead to a situation which is having continuous sparks between the electrodes called arcing and results in severe surface defects. Figure 5 shows the double sparks observed during the experimentation. The maximum spark radius is observed as 62 μm at a maximum capacitance of 2200 nF and voltage of 150 V.

The depth of the crater was measured using Taylor Hobson 3D non-contact profilometer (CCI). Figure 6 shows the three-dimensional and two-dimensional images of the scanned crater cavity at a capacitance of 2200 nF and a voltage of 80 V produced on the test specimen using 3D non-contact profilometer (CCI). The rose color shows the reference level of the image, whereas the red color indicates the ridge formed around the crater cavity. The shape of the crater is analyzed at section Y-Y in Fig. 7.

3.2 EDS analysis of craters

During electric discharge machining, it has been reported that materials can be transferred among the electrodes. The same phenomenon has been observed in the single-spark crater. Hence, in this study, electron dispersion spectroscopy (EDS) analysis is used to identify the elements on the work piece surface. As shown in Fig. 8 and Table 6, tungsten is present on the machined surface, whereas it is not detected on (Fig. 9 and Table 7) the unprocessed surface. It is an evidence for resolidification of molten materials.

Table 6 EDS composition of micro-ED machined Ti-6Al-4V surface

Element	Weight %	Atomic %
Al K	1.77	4.97
Ti K	40.86	64.43
V K	2.67	3.97
Co K	4.78	6.12
W K	49.92	20.51

4 Development of regression models

In order to predict the responses which are driven by the process parameters, an interpolation equation for the response (spark radius) was developed using regression analysis. Simple linear regression is the simplest of the regression models that represent the relationship between the responses and regressors, and it is shown in Eq. (1)

$$z = \beta_0 + \beta_1 x + e \tag{1}$$

where z is the response, β_0 is the constant, β_1 is the coefficient, x is the regressor variable, and e is the random error. Multiple regression models were used to find out the impact of multiple regressors on the responses and often take the form as shown in Eq. (2)

$$z = \beta_0 + \beta_1 x_1 + \beta_2 x_2 + \beta_{12} x_1 x_2 + \beta_{11} x_1^2 + \beta_{22}^2 + e \tag{2}$$

Here, the response z is modeled as the combination of linear, interaction, and quadratic terms of regressor variables x_1 and x_2. β_0 is the constant. β_1, β_2, β_{12}, β_{11}, and β_{22} are the coefficients of the model terms. Experimental errors were included in the model as random error e. In the present study, the spark radius was modeled as a function of voltage and

Table 7 EDS composition of unprocessed Ti-6Al-4V surface

Element	Weight %	Atomic %
Al K	5.88	9.98
Ti K	91.45	86.05
V K	2.67	3.97

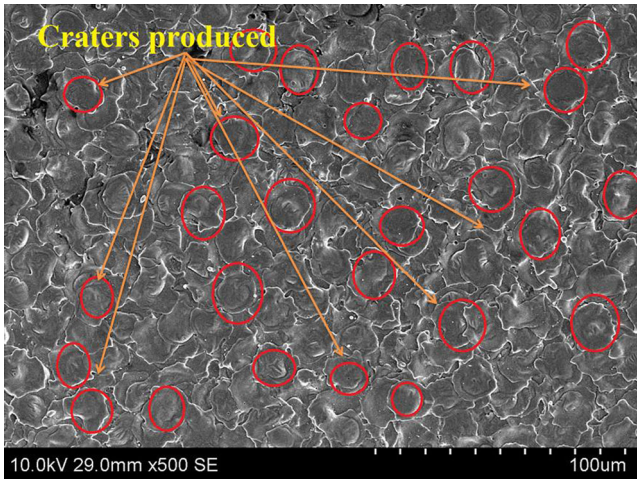

Fig. 10 SEM images of craters on the micro-ED machined surface

capacitance. Multiple regression analysis was performed in Design-Expert software version 9 on the experimental data sets, and the model adequacy was tested using analysis of variance. All variations of models (linear, interaction, quadratic, and cubic) were analyzed, and the best fit value was selected. The developed model for micro-EDM for predicting the spark radius in actual factors is given in Eq. 3.

$$R_s = 21.47 + (0.026 \times \text{Capacitance}) - (0.046 \times \text{Voltage}) + (1.47 \times 10^{-4} \times \text{Capacitance} \times \text{Voltage}) - (1.27 \times 10^{-5} \times \text{Capacitance}^2) \quad (3)$$

In micro-EDM/EDM, the material is removed from the work piece due to the melting and vaporization of the heat generated during the impingement of sparks. It influences not only the material removal rate but also the topography of the surface generated. It is understood that the spark occurs where the gap between tool and work piece surface asperities is the smallest [36]. The subsequent spark occurs at the next highest peak. This process continues to melt and vaporize the peaks on the work piece surfaces to produce a surface with a surface roughness value [27], i.e., the maximum peak-to-valley height is equal to the radius of the crater produced in the single sparks [4, 37]. Therefore, the crater radius produced during the melting and vaporization of peaks is important to understand the topography of the surfaces produced. Hence, the present model is useful to establish the relationship between the important RC-discharge circuit process parameters and spark radius produced during the single spark. The pictorial representations of the relationship between the crater radius and the produced surface are shown in Fig. 10.

Table 8 Comparison of experimental and predicted single-spark radius

Sl. No.	Capacitance (nF)	Voltage (V)	Crater radius (μm)	
			Experimental results	Predicted results
1	500	115	36.42	34.48
2	1	110	15.925	16.45

4.1 Model validations

To demonstrate the successful prediction of the proposed mathematical model, confirmation experiments were done at a capacitance of 500 nF and voltage of 115 V as well as at a capacitance of 1 nF and a voltage of 110 V. The SEM images of the experiments are shown in Fig. 11. The comparison of the predicted spark radius using the developed model and the experimental results are shown in Table 8. The predicted value R_s showed an overall error of 4.258 %. Thus, this model can be successfully adopted for the prediction of spark radius within the design space.

5 Conclusions

In this study, modeling of single-spark micro-electric discharges on Ti-6Al-4V with tungsten carbide electrode has been performed. Based on the experimental results, a detailed

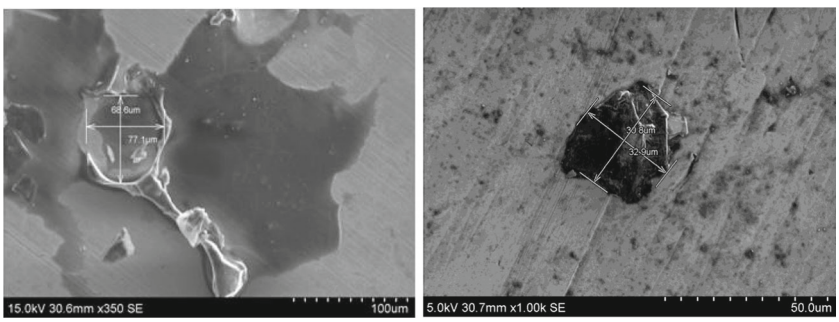

(a) Capacitance of 500nF and a voltage of 115V

(b) Capacitance of 1nF and a voltage of 110V

Fig. 11 SEM images of confirmation experiments. **a** Capacitance of 500 nF and a voltage of 115 V. **b** Capacitance of 1 nF and a voltage of 110 V

parametric study was carried out to study the effect of capacitance and voltage on spark radius. From the analysis, the following conclusions were drawn.

1. Capacitance is the most significant process parameter which influences the spark radius than voltage.
2. Spark radius increases with an increase in capacitance except in the higher energy levels where double sparking phenomenon was observed.
3. In addition to capacitance, interaction of capacitance and voltage as well as the quadratic term of capacitance are also influencing the spark radius (with 95 % confidence level).
4. From the analysis of the surface topography of micro-craters, the shape of the crater is observed as bowl or hemisphere, and also, it is noted that some amount of tool material had been migrated to the work piece surface.
5. Based on regression analysis, a second order regression equation is developed. This model equation is able to predict the spark radius with an accuracy of 95 %.
6. The developed model equation can be successfully adopted for predicting the spark radius of RC-discharge circuit while doing the numerical simulation.

Acknowledgments This paper is a revised and expanded version of a paper entitled "Spark Radius Modeling of Micro Electric Discharge Machining of Ti-6Al-4V" presented at the 5th international and 26th All India Manufacturing Technology, Design and Research conference, AIMTDR2014, IIT Guwahati, India, December 12–14, 2014. The authors gratefully acknowledge the organizing team of AIMTDR2014 for the clearance given for the publication of this paper in IJAMT.

References

1. Jahan MP, Rahman M, Wong YS (2011) A review on the conventional and micro electric discharge machining of tungsten carbide. Int J Mach Tools Manuf 51:837–858
2. Kuriachen B, Somashekhar KP, Mathew J (2014) Multiresponse optimization of micro-wire electrical discharge machining process. Int J Adv Manuf Technol. doi:10.1007/s00170-014-6005-2
3. Jilani ST, Pandey PC (1982) Analysis and modeling of EDM parameters. Precis Eng 4:215–221
4. Dibitonto DD, Eubank PT, Patel MR, Barrufet MA (1989) Theoretical model of the electric discharge machining process. I. The cathode erosion model. J Appl Phys 66:4095–4103
5. Patel MR, Barrufet MA, Eubank PT, Dibitonto DD (1989) Theoretical model of the electric discharge machining process. II. The anode erosion model. J Appl Phys 66:4104–4111
6. Shankar P, Jain VK, Sundararajan T (1997) Analysis of spark profiles during EDM process. Mach Sci Technol 1:195–217
7. Ajit S, Amitabha G (1999) A thermo electric model of material removing during electric discharge machining. Int J Mach Tools Manuf 39:669–682
8. Yu ZY, Kozak J, Rajurkar KP (2003) Modeling and simulation of micro EDM process. CIRP Ann 52:143–146
9. Dhanik S, Joshi SS (2005) Modeling of a single resistance capacitance pulse discharge in micro electro discharge machining. J Manuf Sci Eng 127:759–767
10. Marafona J, Chousal JAG (2006) A finite element model of EDM based on the joule effect. Int J Mach Tools Manuf 46:595–602
11. Joshi SN, Pande SS (2009) Development of an intelligent process model for EDM. Int J Adv Manuf Technol 45:300–317
12. Izquierdo B, Sanchez JA, Plaza S, Pombo I, Ortega N (2009) A numerical model of the EDM process considering the effect of multiple discharges. Int J Mach Tools Manuf 49:220–229
13. Joshi SN, Pande SS (2010) Thermo physical modeling of die sinking EDM process. J Manuf Process 12:45–56
14. Xie BC, Wang YK, Wang ZL, Zhao WS (2011) Numerical simulation of titanium alloy machining in electric discharge machining process. Trans Nonferrous Metals Soc China 21:434–439
15. Shabgard M, Ahmadi R, Seyedzavvar M, Oliaei SNB (2013) Mathematical and numerical modeling of the effect of input-parameters on the flushing efficiency of plasma channel in EDM process. Int J Mach Tools Manuf 65:79–87
16. Izquierdo B, Plaza S, Sanchez JA, Pombo I, Ortega N (2012) Numerical prediction of heat affected layer in the EDM of aeronautical alloys. Appl Surf Sci 259:780–790
17. Zhang Y, Liu Y, Shen Y, Li Z, Ji R, Cai B (2014) A novel method of determining energy distribution and plasma diameter of EDM. Int J heat Mass Transf 75:425–432
18. Yeo SH, Kurnia W, Tan PC (2008) Critical assessment and numerical comparison of electro thermal models in EDM. J Mater Process Technol 203:241–251
19. Snoeys R, Van Dijick FS (1971) Investigation of electro discharge machining operations by means of thermo mathematical model. CIRP Ann 20:35–37
20. Van Dijick FS, Dutre WL (1974) Heat conduction model for the calculation of the volume of molten metal in electric discharges [discharge machining]. J Phys D (Appl Phys) 7:899–910
21. Beck JV (1981) Transient temperatures in a semi-infinite cylinder heated by a disk heat source. Int J Heat Mass Transf 24:1631–1640
22. Jilani ST, Pandey PC (1983) Analysis of surface erosion in electrical discharge machining. Wear 84:275–284
23. Dhanik S, Joshi SS, Ramakrishnan N, Apte PR (2005) Evolution of EDM process modeling and development towards modeling of the micro EDM process. Int J Manuf Technol Manag 7:157–180
24. Yu ZY, Kozak J, Rajurkar KP (2003) Modeling and simulation of micro EDM process. CIRP Ann Manuf Technol 52:143–146
25. Murali MS, Yeo SH (2005) Process simulation and residual stress estimation of micro electric discharge machining using finite element method. J Appl Phys 44(7A):5254–5263
26. Yeo SH, Kurnia W, Tan PC (2007) Electro thermal modeling of anode and cathode in micro EDM. J Phys D 40(8):2513
27. Kiran KMP, Joshi SS (2007) Modeling of surface roughness and the role of debris in micro-EDM. J Manuf Sci Eng 129(2):265–273
28. Allen P, Chen X (2007) Process simulation of micro electro discharge machining on molybdenum. J Mater Process Technol 186: 346–355
29. Mathew J, Allesu K, Srisailam S, Somashekar KP, Prakash Naidu P, Suvin PS (2012) Estimation of residual stress and crater shape in μ-EDM by finite element method. Proceedings of 7th ASME International conference, Texas, USA
30. Somashekhar KP, Mathew J, Ramachandran N (2012) Electrothermal theory approach for numerical approximation of the μ-EDM process. Int J Adv Manuf Technol 61:1241–1246
31. Somashekhar KP, Panda S, Mathew J, Ramachandran N (2013) Numerical simulation of micro-EDM model with multi-spark. Int J Adv Manuf Technol. doi:10.1007/s00170-013-5319-9
32. Tan PC, Yeo SH (2008) Modeling of overlapping craters on micro-electrical discharge machining. J Phys D 41(20):205302

33. Karthikeyan G, Garga AK, Ramkumar J, Dhamodaran S (2012) A microscopic investigation of machining behavior in ED-milling process. J Manuf Process 14:297–306
34. Yoo BH, Min BK, Lee SJ (2010) Analysis of the machining characteristics of EDM as functions of the mobilities of electrons and ions. Int J Precis Eng Manuf 11(4):629–632
35. Jahan MP, Wong YS, Rahman M (2010) A study on the quality micro-hole machining of tungsten carbide by micro-EDM process using transistor and RC-type pulse generator. J Mater Process Technol 209:1706–1716
36. Luo UF (1995) The dependence of interspace discharge transitivity upon the gap debris in precision electrodischarge machining. J Mater Process Technol 68(2):121–131
37. Chen Y, Mahdivian SM (2000) Analysis of electro-discharge machining process and its comparison with experiments. J Mater Process Technol 104(1–2):150–157